Photo-CIDNP studies on reaction centers of rhodobacter sphaeroides

Prakash, Shipra

4 Ground state electronic structure of active cofactors in *Rhodobacter sphaeroides* reaction centers revealed by ^{13}C photo-CIDNP MAS NMR

4.1 Abstract

Photo-CIDNP MAS NMR studies have been performed on reaction centers (RC) of *Rhodobacter sphaeroides* wild type (WT) that have been selectively isotope labelled using (5-^{13}C)-δ-aminolevulinic acid•HCl in all the BChl and BPhe cofactors at positions C-4,5,9,10,14,15,16 and 20. ^{13}C solid-state CP/MAS NMR and ^{13}C-^{13}C dipolar correlation photo-CIDNP MAS NMR provides insight into the ground state electronic structure of the cofactors involved in the electron transfer process in the RC at the atomic scale. The ^{13}C-^{13}C dipolar correlation spectra reveal three strong components assigned to two BChls, P1 and P2, and one BPhe, Φ_A. There is in addition a weak component observed assigned to another BChl, denoted as P3. In the BChls the electron spin density appears to be strongly delocalised over P1 and P2. An almost complete assignment of all the carbon atoms in the aromatic systems of BChl and BPhe has been achieved in combination with previous photo-CIDNP studies on site-directed BChl/BPhe labelled RC (Schulten et al., 2002). The entire ground state electronic structure of all the photochemically active cofactors has been effectively mapped for the first time. One BChl, P2 has well distinguished chemical shifts among the photochemically active BChls suggesting a 'special' BChl. The other two BChls P1 and P3 have similar chemical shifts as BChl *a* in solution and are quite normal. The reason for the anomaly of P2 is discussed.

4.2 Introduction

Photosynthesis in purple bacteria is driven by light-induced electron transfer in the reaction center protein (RC) located in the intracytoplasmic membrane RC of *Rhodobacter (Rb.) sphaeroides* wild type (WT). The RC is a transmembrane protein complex consisting of three polypeptide chains H, M and L and nine cofactors (Yeates et al., 1988; Ermler et al., 1994; Camara-Artigas et al., 2002) (for review, see (Hoff and Deisenhofer, 1997)). Four BChl molecules, two BPhe molecules, two ubiquinones (Q) and a non-heme ferrous iron (Fe^{2+}) are arranged in two nearly symmetric branches (Figure 4.1). The initial process of electron transfer takes place via the "active" A-branch while the B-branch is "inactive". It is generally believed that the primary donor is the 'special pair' (P), a dimer formed of two strongly

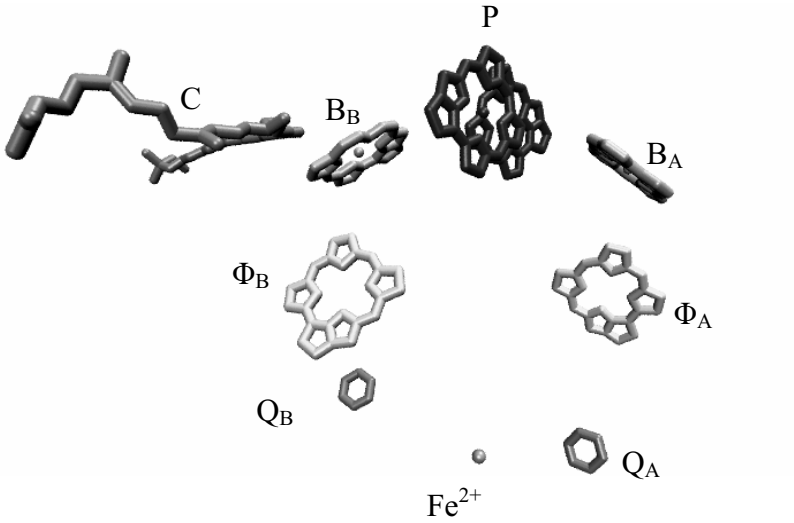

Figure 4.1. Detailed view of the cofactor arrangement in the RC of *Rb. sphaeroides* WT. The aliphatic chains from BChl, BPhe and Q are omitted for clarity.

coupled BChl cofactors P_L and P_M. The primary acceptor is a BPhe molecule, Φ_A. The remaining two accessory BChls, B_A and B_B, are monomers. The tenth cofactor in *Rb. sphaeroides* WT is a carotenoid molecule (C) that breaks the overall symmetry of the cofactor arrangement. It is located near B_B.

After photochemical excitation of P to P*, an electron is transferred to the primary electron acceptor Φ_A within 3 ps, forming the radical pair state $P^{+\bullet}\Phi_A^{-\bullet}$. In the next step, an electron is transferred to the primary quinone acceptor Q_A in about 200 ps. Subsequently, an electron is transferred from Q_A to the final acceptor Q_B. In quinone-depleted reaction centers, the forward transfer from BPhe to Q_A is blocked.

It has been proposed that the excited state P* is electronically asymmetric with more electron density centered on P_M. This electronic asymmetry may be related to the hydrogen-bonding environment of the keto groups (Moore et al., 1999). The electronic structure of the cation radical P^+ has been extensively investigated with EPR, ENDOR and TRIPLE resonance studies (Lendzian et al., 1993; Rautter et al., 1994; Lubitz et al., 2002). The studies have shown that the unpaired electron is unequally distributed over P_L and P_M favoring P_L with a ratio of 2:1. This agrees well with photo-CIDNP MAS NMR investigations on RCs from *Rb. sphaeroides* (WT) reporting a ratio of electron spin density 3:2 in favour of P_L (Chapter 2). The knowledge of P in the electronic-ground state is limited. Resonance Raman studies suggest differences with P_L and P_M in the special pair (Mattioli et al., 1991; Palaniappan et al., 1993) but no details are known.

The involvement of accessory BChl B_A molecule as a real intermediate in the electron transfer to Φ_A has been a matter of debate (for review, see: (Hoff and Deisenhofer, 1997) Absorbance difference spectroscopy with femtosecond time resolution did not see any

involvement of B_A (Martin et al., 1986). On the other hand, transient femtosecond measurements found a biphasic kinetics which could only be interpreted as a two-step model of electron transfer suggesting the involvement of B_A. (Holzapfel et al., 1989, 1990; Holzwarth and Muller, 1996) Subpicosecond transient measurements however have suggested that both, the two-step hopping and the one-step superexchange model of ET may co-exist (Chan et al., 1991). Recently, both these mechanisms have found relevance in the development of molecular wires (Weiss et al., 2004). There has also been a suggestion for a pathway of electron transfer that does not involve the excited state of the special pair dimer (P*), but instead is driven by the excited state of the monomeric BChl (B_A*) (van Brederode et al., 1999). An alternative interpretation based on spin couplings suggest electron transfer from P* to $P^{+\bullet}\Phi_A^{-\bullet}$ with the involvement of a trip-trip-singlet $B^TB_A{}^T$ as a real intermediate between the excited charge separated P* state and the primary charge separated, $P^{+\bullet}\Phi_A^{-\bullet}$(Fischer et al., 1992).

Magic-Angle Spinning (MAS) solid-state NMR is a powerful tool for studying structure and dynamics of membrane proteins (de Groot, 2000). Photochemically induced dynamic nuclear polarization (photo-CIDNP) MAS NMR in combination with site-directed ^{13}C-labeled BChl/BPheo RCs provides an opportunity to study the ground state electronic structure of the cofactors involved in the electron transfer process with atomic selectivity. Photo-CIDNP was observed for the first time in a field of 9.4 T for quinone-blocked frozen bacterial reaction centers (RCs) of *Rhodobacter sphaeroides* R26 using continuous illumination with white light, allowing an enhancement factor of about 200 till 1000 and WT (Zysmilich and McDermott, 1994, 1996b, 1996a; Matysik et al., 2000b; Matysik et al., 2001a; Schulten et al., 2002). Studies on photosystem I of spinach lead to an almost complete set of assignments of the aromatic ring carbons to the P2 cofactor of the primary electron donor P700 (Alia et al., 2004b). In the D1D2 complex of the RC of the photosystem II of plants, observation of the pronounced electron density on rings III and V by photo-CIDNP MAS NMR was taken as an indication for a local electric field, leading to a hypothesis about the origin of the remarkable strength of the redox potential of the primary electron donor P680 (Matysik et al., 2000a; Diller et al., 2005). In addition, NMR signals have been also detected in entire membrane-bound bacterial photosynthetic units (>1.5 MDa) (Chapter 5). Recently, it has been shown that photo-CIDNP can overcome the intrinsic insensitivity and nonselectivity of MAS NMR spectroscopy by enhancing the NMR intensities by a factor of 10000 at a field strength of 4.7 T (Chapter 2).

For the RCs from WT, photo-CIDNP has been described by a combination of two mechanisms (Jeschke and Matysik, 2003) (Chapter 2). In the electron-electron-nuclear three-spin mixing (TSM) mechanism, net nuclear polarization is created in the spin-correlated radical pair due to the presence of both anisotropic hyperfine interaction and coupling between the two electron spins (Jeschke, 1998). In the Differential Decay (DD) mechanism, a

net photo-CIDNP effect is caused by anisotropic hyperfine coupling without an explicit requirement for electron-electron coupling if spin-correlated radical pairs have different lifetimes in their singlet and triplet states (Polenova and McDermott, 1999).

Photo-CIDNP MAS NMR in combination with site-directed ^{13}C-labeled BChl/BPheo RCs, labelled at positions C-1,3,6,8,11,13,17,19 in the porphyrin ring, gave the first insight into the ground state electronic structure of the special pair at the atomic scale (Schulten et al., 2002). The studies have shown that two BChls, P1 and P2, have different chemical shift values. This has been interpreted in terms of different electron densities on both cofactors, presumably with higher electron density on P2. In addition, a small fraction of π-spin density was observed on a third BChl, designated as P3 (Schulten et al., 2002).

Photo-CIDNP MAS NMR studies performed on selectively labelled BChl/BPhe RCs, labelled at positions C-4,5,9,10,14,15,16,20, are reported here. These RCs have been prepared using (5-^{13}C)-δ-aminolevulinic acid•HCl as a precursor for BChl/BPhe biosynthesis. 1D CP/MAS and photo-CIDNP MAS NMR experiments confirm the remarkable similarity between the ground state electronic structures before and after illumination. To probe the ground state electronic structure of the cofactors involved in the electron transfer process, ^{13}C-^{13}C dipolar correlation photo-CIDNP MAS NMR experiments on the ^{13}C-labelled BChl/BPhe RCs have been performed. The ^{13}C chemical shifts from these photo-CIDNP studies in combination with previous studies have lead to for the first time, to a comprehensive map of the molecular electronic ground state of the photochemically active cofactors with the atomic selectively.

4.3 Materials and Methods

4.3.1 Sample preparation

Cultures of *Rb. sphaeroides* WT (480 mL) were grown anaerobically in the presence of 1.0 mM (5-^{13}C)-δ-aminolevulinic acid•HCl ($COOHCH_2CH_2{}^{13}COCH_2NH_2$•HCl, 99% ^{13}C-enriched), which was purchased from Cambridge Isotope Laboratories (Andover, USA). Incorporation of (5-^{13}C)-ALA, as reported in this paper, produces BChl and BPhe macrocycles, labeled at the C-4, C-5, C-9, C-10, C-14, C-15, C-16 and C-20 (Figure 4.2). The cultures were grown for 7 days in light. Prior to harvesting the cells for the preparation of RCs, a 4 mL aliquot was taken from the culture and the extent of ^{13}C incorporation of (4-^{13}C)-ALA into BChl has been determined as described in detail earlier (Schulten et al., 2002). The total ^{13}C-label incorporation in BChl/BPhe ($^{13}C_{0\text{-}8}$) was ~ 60±5%. The culture was centrifuged for 10 min at 5500 × g, and the combined pellet was resuspended in 0.1 M phosphate buffer (pH = 7.5). The RCs were isolated as described by (Shochat et al., 1994).

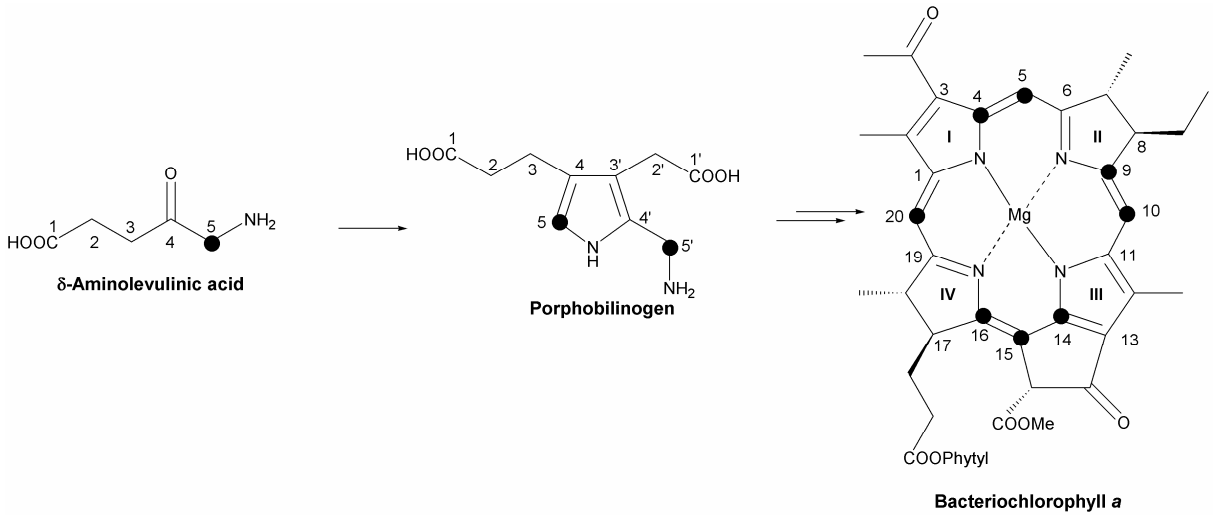

Figure 4.2. Schematic representation of the biosynthesis of BChl *a* and BPhe *a* starting from δ–aminolevulinic acid (ALA). The positions of ^{13}C labels are indicated by filled circles *(●)*. The numbering of BChl *a* is according to the IUPAC nomenclature.

Approximately 15 mg of the labeled RC was reduced with 0.05 M sodium dithionite and used for the NMR experiments.

4.3.2 MAS-NMR Measurements

Photo-CIDNP MAS NMR experiments were performed with a DMX-200 NMR spectrometer equipped with a double-resonance MAS probe operating at 200 MHz for ^{1}H and 50 MHz for ^{13}C. The RC sample was loaded into a clear sapphire 4 mm rotor, and ^{13}C MAS NMR spectra were recorded at a temperature of 223 K and a spinning frequency of 8 kHz. The sample was continuously illuminated during the course of the experiment. The illumination setup has been described in detail in Chapter 1. 1D photo-CIDNP MAS NMR spectra were collected with a Hahn echo-pulse sequence and two pulse-phase modulation (TPPM) proton decoupling. A recycle delay of 4 s was used.^{13}C CP MAS NMR data were obtained with a AV-750 NMR spectrometer. A total of 4k scans were recorded at a temperature of 223 K with a spinning frequency of 12 kHz. For the 2D homonuclear (^{13}C -^{13}C) dipolar correlation spectra, an adapted RFDR pulse sequence was applied with the initial cross polarization step replaced by a $\pi/2$ pulse. The RFDR experiments were recorded with mixing times of 4 and 8 ms. In the t_2 dimension, 2k data points with a sweep width of 50 kHz were recorded. Zero-filling to 4k and an exponential line broadening of 25 Hz were applied prior to Fourier transformation. In the t_1 dimension, 256 scans using 1k data points were recorded. A sine squared apodisation shifted by $\pi/2$ was applied prior to Fourier transformation. All spectra were externally referenced to the $^{13}COOH$ response of solid tyrosine·HCl at 172.1 ppm.

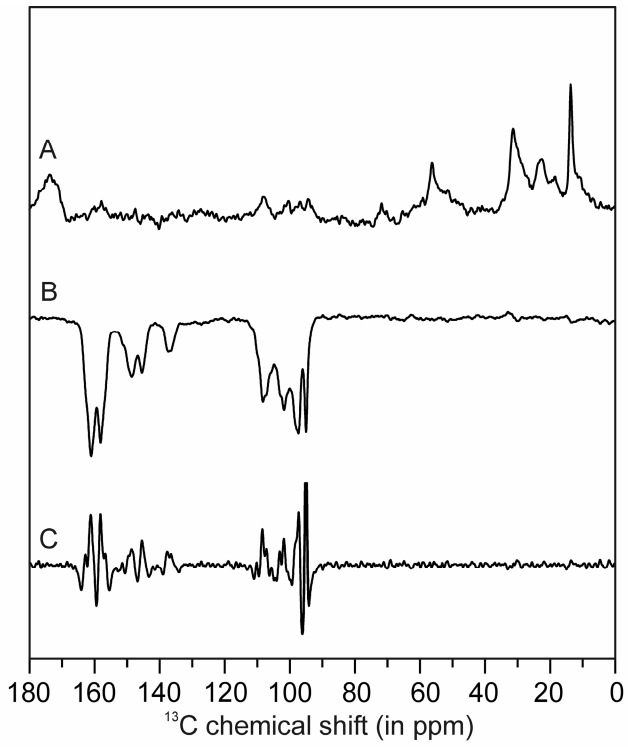

Figure 4.3. 1D solid-state MAS NMR spectra of BChl/Bphe labelled RC of *Rb. sphaeroides* WT. The dark ^{13}C CP/MAS NMR spectrum (A) was recorded at a field strength of 17.6 T at 223 K with a spinning frequency of 12 kHz. The photo-CIDNP spectrum (B) was recorded with continuous illumination in white light at a field strength of 4.7 T and at a temperature of 223 K with a spinning frequency of 8 kHz. Spectrum in (C) is the second derivative of the 1D photo-CIDNP spectrum (B).

4.4 Results and Discussion

4.4.1 Comparison of light with dark spectra

The ^{13}C CP MAS NMR spectrum from labelled RCs obtained in the dark is shown in Figure 4.3A. Several broad natural abundance ^{13}C responses are observed between 10 and 70 ppm from the saturated carbons in the apoprotein and another signal at 173 ppm is observed due to the carbonyl groups in the protein. Weak signals are observed in the region from 90 to 110 ppm corresponding to the response from ^{13}C-enriched BChl and BPhe in the RC. Continuous illumination with white light generates the photo-CIDNP MAS NMR spectrum as shown in Figure 4.3B. Strong emissive peaks appear in the region between 90 ppm to 110 ppm due to the photo-CIDNP from the methine carbons, ^{13}C-5, ^{13}C-10, ^{13}C-15 and ^{13}C-20. In the aromatic region of the spectrum from 135 ppm to 165 ppm the responses from the ^{13}C-4, ^{13}C-9, ^{13}C-14 and ^{13}C-16 are detected. To resolve the responses from the various labelled carbons, the second derivative of the 1D photo-CIDNP spectrum (Figure 4.3B) of the labelled RCs was calculated as shown in Figure 4.3C.

There are photo-CIDNP signals from more than eight carbons indicating that more than a single BChl is polarised. The broad peaks at 108.4, 97.2 and 95.2 ppm in the ^{13}C CP MAS spectrum (Figure 4.3A) are narrower and strongly emissive in the photo-CIDNP spectrum

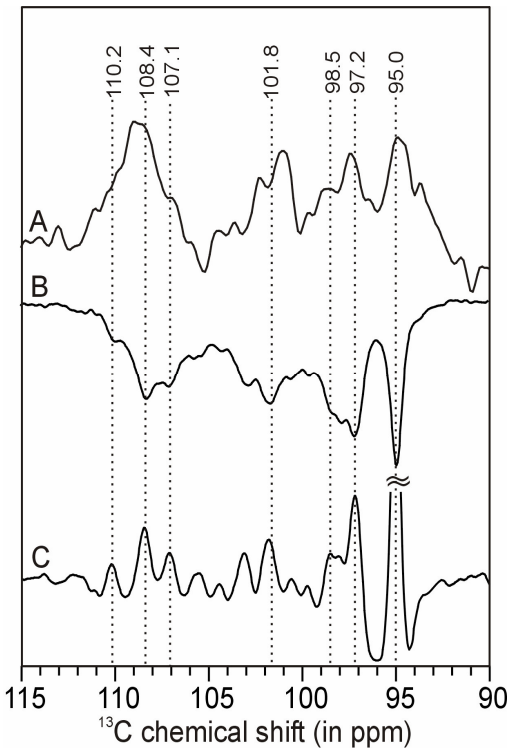

Figure 4.4. Detailed view of the methine region in the spectra in Figure 4.3. In both light and dark spectra the labelled carbons resonate with comparable chemical shifts, visualized by dashed lines.

(Figure 4.3B). These peaks are better resolved by taking the second derivative of the 1D photo-CIDNP spectrum (Figure 4.3C). The chemical shifts of the responses that were recorded in the dark are comparable to the shifts recorded with illumination. A detailed view of the spectra from 90 to 115 ppm is shown in Figure 4.4.

4.4.2 Assignment of the ^{13}C-^{13}C dipolar correlation spectra

To gain information on the ground state electronic structure of the donor molecule, P and the acceptor molecule Φ, 2D RFDR data sets were collected from polarized samples.

The RFDR spectrum (Figure 4.5) was recorded with a mixing time of 4 ms. In the BChl and BPhe rings separated by a single bond, strong correlations appear within each pair of enriched carbons, i.e. C-4/C-5, C-9/C-10, C-14/C-15, and C-15/C-16. In addition cross peaks are observed between C-14/C-16 over a distance of ~2.3 Å. Four sets of correlation networks are visible. Three networks which give strong correlations are assigned to two BChl molecules denoted as P1, P2 and one to BPhe, Φ_A. The fourth network is weak and is assigned to a BChl, denoted as P3.

The NMR shifts for monomeric BChl *a* and BPhe *a* in solution are shown in Table 4.1. The methine carbons in BChl *a* and BPhe *a* in acetone-d_6 resonate between 95 ppm and 110 ppm and the methine shift differences between the BChl and BPhe are 2 ppm or less. Hence, the diagonal peaks in this region can be attributed to the C-5, 10, 15 and 20 and can be used as starting points in the assignment procedure.

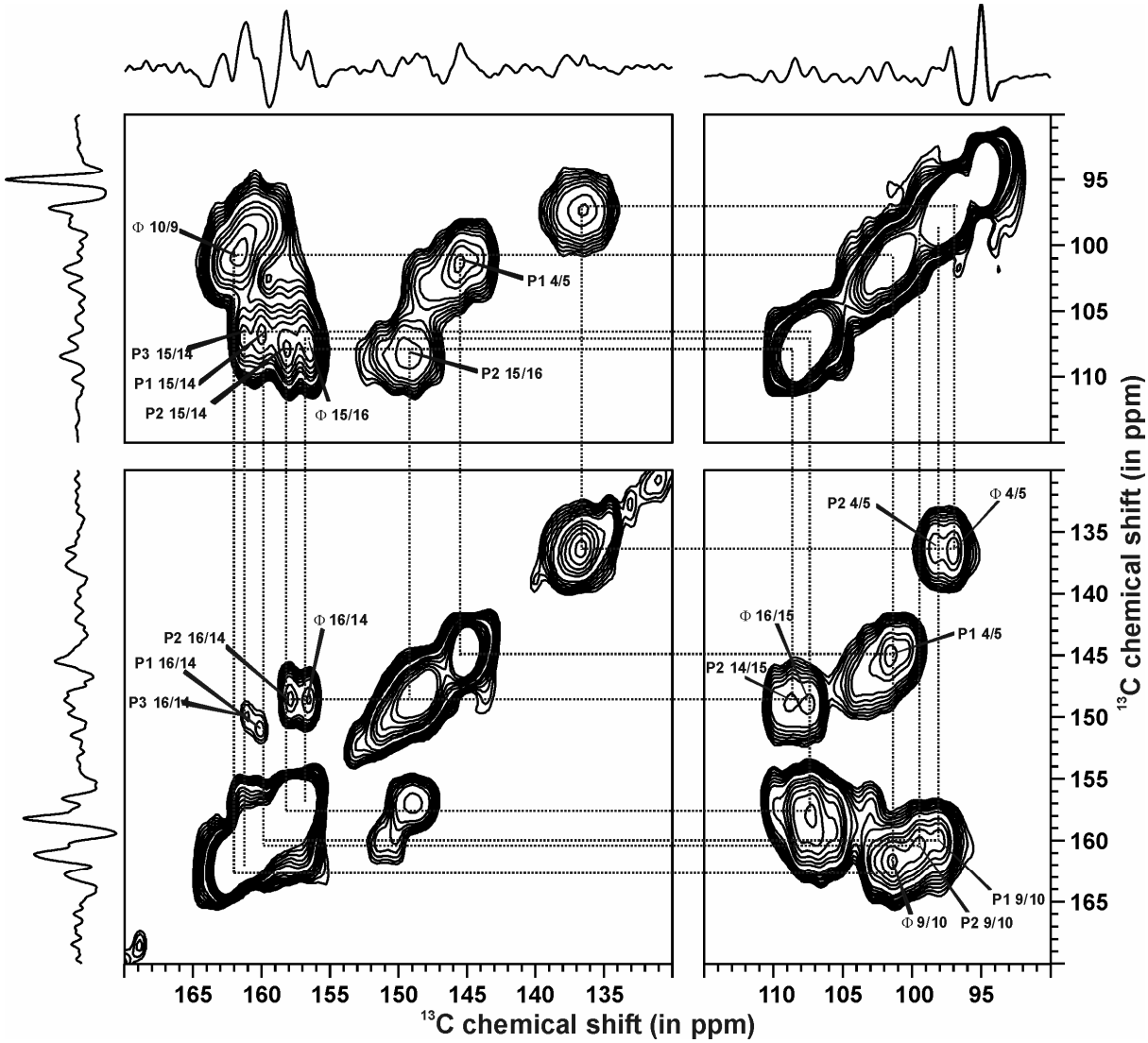

Figure 4.5. Contour plot sections of a ^{13}C- ^{13}C dipolar correlation photo-CIDNP MAS NMR spectrum of ($^{13}C_{0\text{-}8}$ BChl/BPhe)-RCs of *Rb. sphaeroides* WT recorded at a field strength of 4.7 T and 223 K, using a spinning frequency of 8 kHz and a mixing time of 4 ms. The labels refer to the cross peaks for the three BChl correlation networks P1, P2 and P3 and the BPhe component Φ. The upper trace shows parts of the second derivative of 1D photo-CIDNP MAS NMR spectrum.

A major difference in chemical shift of 12.1 ppm between BChl and BPhe is detected for C-4 and 14. The ^{13}C responses of C-14 and C-16 of Φ in acetone d_6 at 148.7 and 158.7 ppm, respectively, overlap with the C-16 and C-14 of BChl at 152.2 and 160.8 ppm, respectively. Three correlations are observed for C-14/C-15 at 160.0/106.8 (P1), 158.0/108.2 (P2) and 161.2/107.1 ppm (P3). A correlation is also observed for C-16/C-15 of Φ at 149.1/107.5 ppm. In addition, correlations are observed for C-16/C-15 of P2 at 148.8/108.2 and C-14/C-15 of Φ at 149.1/107.5 ppm. These assignments are confirmed by cross peaks detected between C-14 of ring III and C-16 of ring II. Two strong correlations are observed for C-14/C-16 at 158.0/148.8 ppm (P2) and for C-16/C-14 at 149.1/156.6 ppm (Φ). In addition, two weak correlations are observed for C-14/C-16 at 160.0/151.4 ppm (P1) and at

carbon no.	BChl *a*				BPhe *a*	
	σ_{liq} [a]	P1[b]	P2[b]	P3[b]	σ_{liq} [a]	Φ[b]
1	150.8	148.2	143.4	148.5	139.7	138.3
3	137.4	130.2	127.6	133.2	134.8	134.7
4	150.2	145.4	136.8		138.1	136.8
5	99.6	101.6	98.4		98.4	97.2
6	168.4	166.8	164.6	167.0	170.9	171.1
8	55.6	53.0	55.4	50.6	55.4	54.6
9	158.5	160.2	161.0		164.3	162.2
10	102.4	98.1	99.6		100.4	101.5
11	149.4	150.3	154.2	149.4	139.3	138.9
13	130.3	131.0	131.3	130.2	129.3	126.4
14	160.8	160.0	158.0	161.2	148.7	149.1
15	109.7	106.8	108.2	107.1	109.9	107.5
16	152.2	151.4	148.8	150.3	158.7	156.6
17	50.4	47.3	49.7	48.7	51.5	52.5
19	167.1	162.5	159.7	162.7	169.8	169.9
20	96.3				97.6	

[a] The liquid NMR chemical shift data σ_{liq} have been obtained in acetone-d_6.
[b] Assignment for carbons 1,3,6,8,11,13,17 and 19 from (Schulten et al., 2002).

Table 4.1. Chemical shifts of monomeric BChl a and BPhe a cofactors.

161.2/150.3 ppm (P3). The ^{13}C response of C-4 of Φ in acetone-d_6 at 138.1 ppm is very different from the ^{13}C response of C-4 of BChl at 150.2 ppm. A correlation is detected at 136.8/97.2 ppm which is assigned to C-4/C-5 of Φ.

There is another C-4/C-5 correlation observed at 136.8/98.4 ppm which cannot be assigned to a Φ, since only one Φ is present in the active branch. This can only be assigned to a C-4/C-5 correlation of BChl revealing an upfield shifted C-4 by 13.4 ppm. Previously 2D photo-CIDNP MAS NMR studies on BChl/BPhe ($^{13}C_{0-8}$)-RCs, with a different labeling pattern, have shown that the ^{13}C responses from ring I carbons of P2 are upfield shifted by 10.2 and 7.4 ppm respectively (Schulten et al., 2002). ^{13}C responses from ring I carbons of P1 are also upfield shifted but to a smaller extent. Thus the C-4/C-5 correlation at 136.8/98.4 ppm is assigned to P2. Another correlation observed at 145.4/101.6 ppm, is assigned to C-4/C-5 of P1.

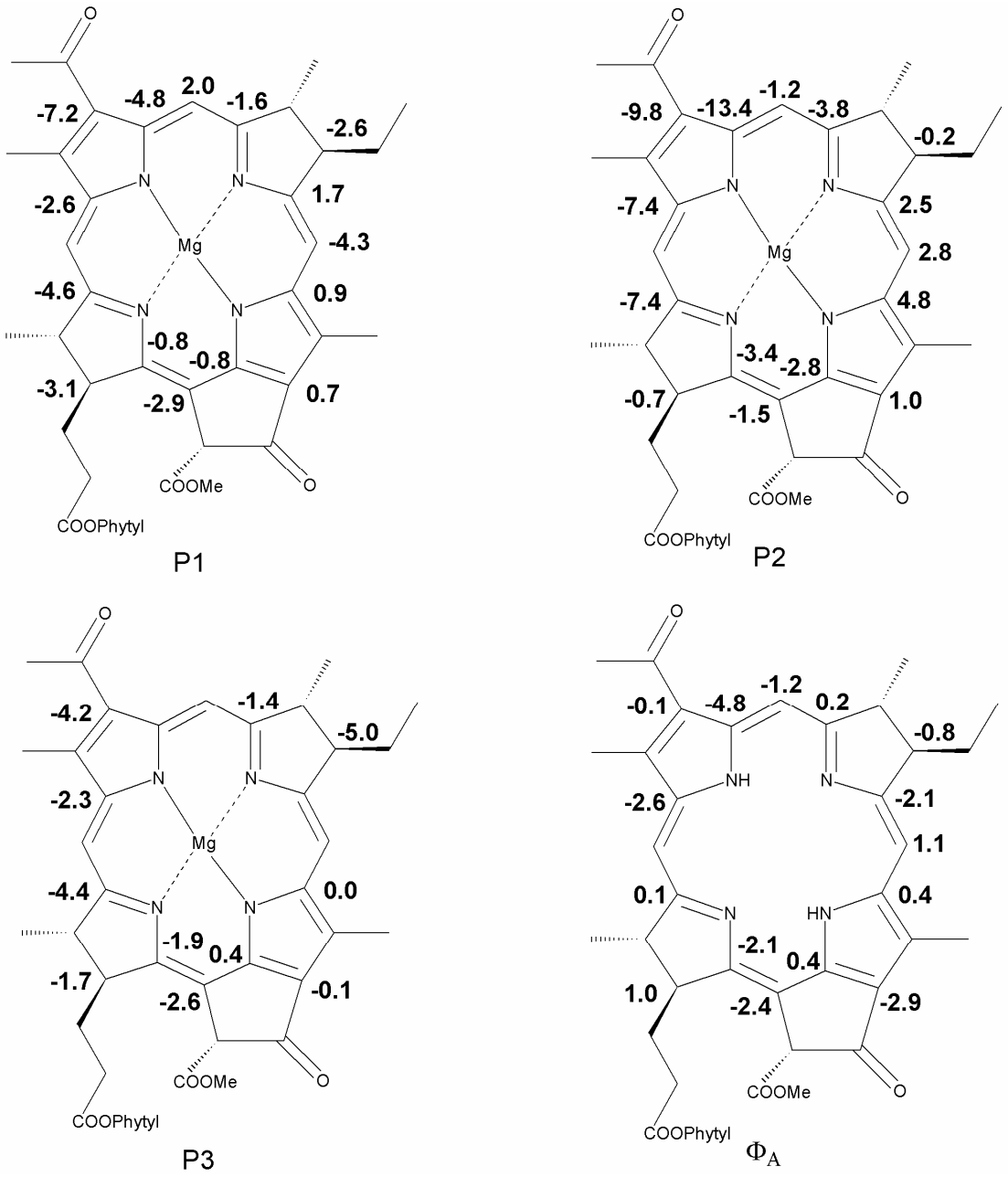

Figure 4.6. Detected chemical shift differences $\Delta\sigma = \sigma_{ss}-\sigma_{liq}$ for the three BChls P1, P2, P3 and the BPhe Φ_A.The positive values denote an upfield and the negative values a downfield shift.

Finally, a correlation is observed for C-9/C-10 of Φ at 162.2/101.5 ppm. The ^{13}C response from C-9 of BChl overlaps with ^{13}C response of C-14 of BChl. Cross peaks observed between C-9/C-10 of P2 at 161.0/99.6 and at 160.2/98.1 for P1 make it possible to assign C-9. The complete list of the ^{13}C assignments for all the photochemically active cofactors is presented in Table 4.1. ^{13}C assignments from previous photo-CIDNP MAS NMR studies are also shown in Table 4.1 to build a comprehensive map of the electronic ground state structure of the photochemically active cofactors (Schulten et al., 2002). Since no correlations are observed for C-9/C-10, C-4/C-5 for P3, it was not possible to make these assignments. The same is also

true for C-20 for which no cross peaks were seen. Comparing the chemical shifts of P1, P2 and P3, it can be concluded that P2 is 'special' among them.

Protein-pigment upfield shifts are observed for several carbons of P1, P2 and P3 (Table 4.1). The chemical shift differences $\Delta\sigma = \sigma_{ss} - \sigma_{liq}$ for the three BChls P1, P2, P3 and one BPhe Φ_A are shown in Figure 4.6. The BPhe Φ_A, exhibits both upfield and downfield shifts of < 3 ppm except for carbon C-4 which shows an upfield shift of 4.8 ppm. In the BChls P1, P2 and P3, the carbons around rings I and IV are upfield shifted as compared to other carbons. Pronounced upfield shifts are observed for P2 in the pyrrole ring I as compared to P1 and P3. This effect is clearly visible in the carbons C-1, C-3 and C-4 of P2, upfield shifted by 7.4, 9.8 and 13.4 ppm respectively. On the other hand, for P1 and P3, carbons around rings I and IV are upfield shifted by 2-7 ppm. The two BChls P_L and P_M of P overlap over ring I. Ring current shifts could therefore explain the strong upfield shifts around ring I for P2. However, ring current shifts are less than ~ 3 ppm and therefore cannot explain upfield shifts in the range of 7-13 ppm.

4.4.3 Identity of the cofactors

The pronounced upfield shifts in ring I of P2 suggest strong interactions in the vicinity of the photochemically active cofactors, that is P (P_L and P_M) and B_A.There are many polar amino acid residues surrounding the cofactors. The large upfield shifts could be explained by a strong interaction like a hydrogen bond to one of the amino acid residues. The X-ray structure of the RC reveals that a histidine residue (His L168) is located near the 3-acetyl group of P_L (Figure 4.7). Resonance Raman studies have already given evidence that a hydrogen bond exists at 3-acetyl group of P_L (Mattioli et al., 1991). In addition, site-directed mutants at positions His L168 and Phe M197 also have shown that an addition of a hydrogen bond can be correlated with an increase of the dimer midpoint potential (Lin et al., 1994). The appearance of the upfield shifts in ring I of P2 could then be tentatively assigned to the local hydrogen bonding between the acetyl carbonyl and the NH of the imidazole side chain of His L168. This leads to the assignment of P2 to BChl P_L located at the active A-branch. The other strong BChl component P1 is assigned to P_M and the weak component P3 is assigned to the accessory BChl B_A. The different chemical shifts of P_L in comparison to P_M and B_A indicate a 'special' local electronic environment in the ground state around P_L. The upfield shift of 13.4 ppm on C-4 of P_L indicates a stabilization of ~ -0.08 electronic equivalent negative charge on this atom relative to the monomer in solution. Strong upfield shifts around ring I of P_L, to a lesser extent around ring IV, suggest a localisation of the electronic charge over these rings primarily. The role of His L168 may be is to stabilise the charge on P_L. The comprehensive map of the electronic ground state of the special pair confirms previous results that P is asymmetric already in the ground state with excess negative charge on P_L. The functional asymmetry in the RC is thus introduced in the ground state.

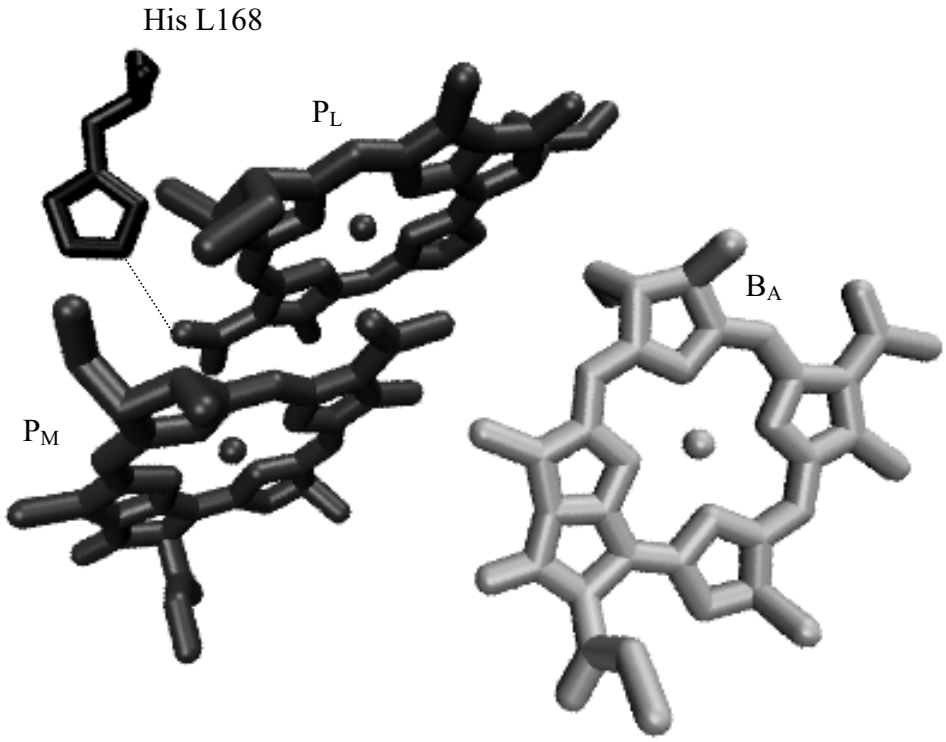

Figure 4.7. View from the top of the special pair, P_L and P_M and the accessory BChl B_A. His L168 in the back interacts with the 3-acetyl group of P_L.